

Coherent Control of Magneto-optical Rotation

Anil K. Patnaik and G. S. Agarwal

Physical Research Laboratory, Navrangpura, Ahmedabad-380 009, India

(March 1, 2000)

The contribution from the magnetic sublevels of a medium produce birefringence in presence of magnetic field resulting in the rotation of the plane of polarization of a weak probe field. We show how the rotation of plane of polarization, due to the magnetic field, can be controlled by a laser tuned close to a nearby transition. We include the inhomogeneous broadening. We present analytical results for the susceptibilities corresponding to the two circular polarization components of the probe field. We identify the region of parameters where very significant enhancement of magneto-optical rotation can be obtained. The control field opens up many new regions of the frequencies of the probe where large magneto-optical rotation occurs.

PACS no. 42.50.Gy, 33.55.Ad, 42.25.Lc

I. INTRODUCTION

A magnetic field, when applied to an initially isotropic medium containing gaseous atoms having m -degenerate sublevels, can cause birefringence in the medium. Because, the applied magnetic field creates asymmetry between the susceptibilities χ_{\pm} of the medium corresponding to the two circularly polarized components σ_{\mp} of the probe field. That results in magneto-optical rotation (MOR), i.e. a linearly polarized weak probe passing through a medium has its plane of polarization is rotated. For a small absorption the rotation angle θ is given by (Fig.1)

$$\theta = \pi k_p l (\chi_- - \chi_+) ; \quad (1)$$

where \vec{k}_p corresponds to propagation vector of the probe and l is length of the cell along \vec{k}_p . Further we note that, χ_{\pm} depend on the atomic density and the oscillator strength of the atomic transition. Extensive literature on MOR exists [1–6] including several interesting applications. The MOR with saturating fields is discussed in [5,6]. Several studies have also reported birefringence induced by the application of a laser field [7–9]. Wielandy and Gaeta [9] demonstrated the possibility of controlling the polarization state of the probe field using an additional laser field. The use of additional laser fields to control the optical properties of the system has been extensively discussed in the literature [4,10] and in this paper we report how magneto-optical rotation can be controlled by laser fields. We will present results for both homogeneously [11] and Doppler broadened cases.

The organization of the paper is following. In Sec II, we describe the model system for producing enhancement of MOR. We present the density matrix equation. In Sec.III we consider the atomic response to a weak probe field and derive analytical expressions for the susceptibilities of the Doppler broadened medium. In Sec.IV, we give a measure of rotation of the plane of polarization. In Sec.V, we show how one identifies the regions of interest and demonstrate how the birefringence can be

controlled efficiently. Thus large enhancement in MOR can be obtained by suitably choosing the control field parameters. Our work demonstrates the possibility of realizing a magneto-optical switch, that switches given polarization state of the probe to its orthogonal component [12]. We conclude with a summary of the results in Sec.VI.

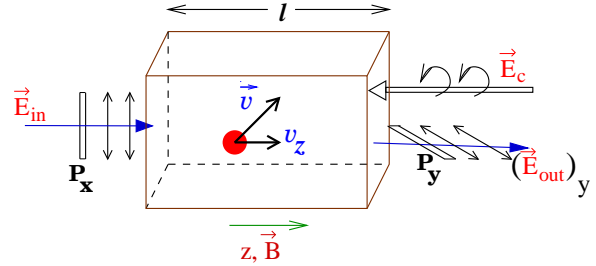


FIG. 1. The configuration under consideration which gives rise to significantly large MOR and large enhancements. The direction of magnetic field \vec{B} fixes quantization axis (z -axis). The control field (\vec{E}_c) and the input probe field (\vec{E}_{in}) are counter propagating along the z -axis. The atom in the cell moves with velocity \vec{v} in arbitrary directions. P_x and P_y are x -polarizer at input and y -polarized analyzer at the output respectively. $(\vec{E}_{out})_y$ is the output probe after passing through P_y .

II. THE MODEL AND THE SUSCEPTIBILITIES

The MOR consists of the propagation of linearly polarized light \vec{E}_p tuned close to the transition $j \leftrightarrow j'$ in presence of a magnetic field \vec{B} . The susceptibilities χ_{\pm} for the two circularly polarized components of the probe beam would be different as $\vec{B} \neq 0$. We can now consider the role of a control field \vec{E}_c which can be tuned close to another transition say $j'' \leftrightarrow j'''$. In this paper we study how the control field induced modification of χ_{\pm} can lead to large MOR. In what follows, we consider a special case

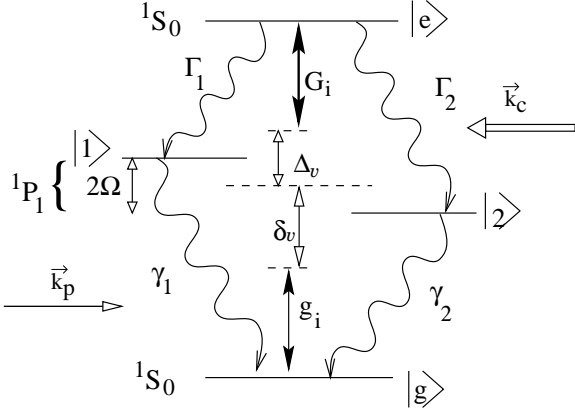


FIG. 2. The four-level model scheme having m -degenerate sub-levels $|1\rangle$ and $|2\rangle$ as its intermediate states. The magnetic field \vec{B} gives rise to Zeeman splitting 2Ω . The symbols in the left hand side depict the energy levels of ^{40}Ca atom. The spontaneous decay rates are denoted by $2\Gamma_i$ and $2\gamma_i$. The probe field (\vec{k}_p) and the control field (\vec{k}_c) are counter propagating. The Rabi frequencies of probe field and the control field are given by $2g_i$ and $2G_i$, corresponding to the $|i\rangle \leftrightarrow |g\rangle$ and $|e\rangle \leftrightarrow |i\rangle$ couplings respectively ($i = 1, 2$). The detunings of the probe and control fields from the degenerate $j = 1$ state, in the moving atomic frame of reference, are δ_v and Δ_v respectively.

($j = 0, j' = 1, j'' = 0$), which leads to the set shown in Fig.2. This scheme, for example, is relevant to level configuration of ^{40}Ca . In our calculation, we have ignored the $j = 0, m = 0 \leftrightarrow j = 1, m = 0$ transitions; which assumes that the loss of population to/from $m = 0 \leftrightarrow m = 0$ states due to spontaneous emission can be pumped back by incoherent pumping. Further, \vec{E}_c and \vec{E}_p are taken to be counter propagating along z . We write the fields in the circular basis as

$$\vec{E}_\alpha = (\mathcal{E}_{\alpha+}\hat{\epsilon}_+ + \mathcal{E}_{\alpha-}\hat{\epsilon}_-) e^{i\vec{k}_\alpha \cdot \vec{r} - i\omega_\alpha t}, \quad \alpha = c, p; \quad (2)$$

where

$$\hat{\epsilon}_\pm = \frac{\hat{x} \pm i\hat{y}}{\sqrt{2}}. \quad (3)$$

Here $\mathcal{E}_{c\pm}$ ($\mathcal{E}_{p\pm}$) represent the σ_\mp components of the control field (probe field). Let the dipole matrix elements corresponding to $|e\rangle \leftrightarrow |i\rangle$ and $|i\rangle \leftrightarrow |g\rangle$ transitions be represented by \vec{D}_{ei} and \vec{d}_{ig} respectively. The polarization state of the incident fields decide the various field couplings between the $j = 0 \leftrightarrow j = 1 \leftrightarrow j = 0$ states. The dipole matrix elements \vec{D}_{ij} and \vec{d}_{ij} can be written with their corresponding Clebsch-Gordan coefficients as

$$\begin{aligned} \vec{D}_{e1} &= -D\hat{\epsilon}_+, \quad \vec{D}_{e2} = D\hat{\epsilon}_-, \\ \vec{d}_{1g} &= -d\hat{\epsilon}_-, \quad \vec{d}_{2g} = d\hat{\epsilon}_+; \end{aligned} \quad (4)$$

where D (d) denotes the reduced dipole matrix element corresponding to upper (lower) $j = 0 \leftrightarrow j = 1$ ($j = 1 \leftrightarrow j = 0$) transitions.

In the rotating wave approximation, the interaction Hamiltonian \mathcal{H}_1 is

$$\begin{aligned} \mathcal{H}_1(t) = & -\hbar \sum_{i=1,2} [|i\rangle \langle g| g_i e^{-i\omega_p t + i\vec{k}_p \cdot \vec{v}t} \\ & + |e\rangle \langle i| G_i e^{-i\omega_c t + i\vec{k}_c \cdot \vec{v}t} + H.c.]; \end{aligned} \quad (5)$$

where Rabi frequencies $2G_i$ and $2g_i$ of the control and probe lasers are

$$G_i = \frac{\vec{D}_{ei} \cdot \vec{E}_c}{\hbar}, \quad g_i = \frac{\vec{d}_{ig} \cdot \vec{E}_p}{\hbar}. \quad (6)$$

On combining Eq.(4) and (6) we obtain,

$$\begin{aligned} G_1 &= -\frac{D\mathcal{E}_{c-}}{\hbar}, \quad G_2 = \frac{D\mathcal{E}_{c+}}{\hbar}, \\ g_1 &= -\frac{d\mathcal{E}_{p+}}{\hbar}, \quad g_2 = \frac{d\mathcal{E}_{p-}}{\hbar}. \end{aligned} \quad (7)$$

In terms of Fig.2, the unperturbed Hamiltonian \mathcal{H}_0 is

$$\begin{aligned} \mathcal{H}_0 = & \hbar(\omega_{eo} + \omega_{og})|e\rangle \langle e| + \hbar(\omega_{og} + \Omega)|1\rangle \langle 1| \\ & + \hbar(\omega_{og} - \Omega)|2\rangle \langle 2|, \end{aligned} \quad (8)$$

where the index o represents the dashed level in Fig.2. We work with the density matrix framework as this can account properly all spontaneous emission processes. The atomic dynamics is described by the master equation

$$\begin{aligned} \dot{\rho} = & \frac{-i}{\hbar} [\mathcal{H}_0 + \mathcal{H}_1(t), \rho] - \sum_{i=1,2} (\Gamma_i \{|e\rangle \langle e|, \rho\} + \gamma_i \{|i\rangle \langle i|, \rho\} \\ & - 2\Gamma_i \rho_{ee} |i\rangle \langle i| - 2\gamma_i \rho_{ii} |g\rangle \langle g|). \end{aligned} \quad (9)$$

The second term under the summation sign represents the natural decays of the system. The Γ 's and γ 's represent various natural line widths, and the curly bracket represents the anti-commutator. The explicit time dependence can be eliminated by making a transformation $\rho \rightarrow \tilde{\rho}$ such that

$$\begin{aligned} \tilde{\rho}_{ii} &= \rho_{ii}, \quad \tilde{\rho}_{ig} = \rho_{ig} e^{i\omega_p t - i\vec{k}_p \cdot \vec{v}t}, \\ \tilde{\rho}_{ei} &= \rho_{ei} e^{i\omega_c t - i\vec{k}_c \cdot \vec{v}t}, \quad \tilde{\rho}_{eg} = \rho_{eg} e^{i(\omega_p + \omega_c)t - i(\vec{k}_p + \vec{k}_c) \cdot \vec{v}t}. \end{aligned} \quad (10)$$

The matrix equation for $\tilde{\rho}$ is found to be

$$\begin{aligned} \dot{\tilde{\rho}} = & \frac{-i}{\hbar} [\tilde{\mathcal{H}}, \tilde{\rho}] - \sum_{i=1,2} (\Gamma_i \{|e\rangle \langle e|, \tilde{\rho}\} + \gamma_i \{|i\rangle \langle i|, \tilde{\rho}\} \\ & - 2\Gamma_i \rho_{ee} |i\rangle \langle i| - 2\gamma_i \rho_{ii} |g\rangle \langle g|), \end{aligned} \quad (11)$$

with

$$\begin{aligned} \tilde{\mathcal{H}} = & \hbar(\delta_v + \Delta_v)|e\rangle \langle e| + \hbar(\delta_v + \Omega)|1\rangle \langle 1| + \hbar(\delta_v - \Omega)|2\rangle \langle 2| \\ & - \hbar \sum_{i=1,2} \{g_i |i\rangle \langle g| + G_i |e\rangle \langle i| + H.c.\}; \end{aligned} \quad (12)$$

where

$$\begin{aligned}\delta_v &= \delta + k_p v_z, \quad \Delta_v = \Delta - k_p v_z; \\ k_p &\approx k_c; \quad \Delta_v + \delta_v \approx \Delta + \delta.\end{aligned}\quad (13)$$

Here $\delta = \omega_{og} - \omega_p$, $\Delta = \omega_{eo} - \omega_c$ correspond to the detunings of the probe and control field when the atom is stationary. The susceptibilities of the medium corresponding to the different polarization components of the probe field, can be expressed in terms of the off-diagonal density matrix elements. Therefore χ_{\pm} is obtained by solving Eq.(11). Here, in the following, we outline the calculation and present analytical results.

Let χ_+ (χ_-) be the susceptibilities of the moving atom to the σ_- (σ_+) component of the probe field. We choose the probe field polarization such that $g_i \neq 0$. One can write χ_{\pm} in terms of dimensionless quantities as

$$\chi_{\pm} = \left(\frac{\alpha}{4\pi k_p} \right) s^{\pm}; \quad (14)$$

where s^{\pm} , the normalized susceptibilities are given by

$$s^+ = \left(\frac{\tilde{\rho}_{1g}\gamma}{g_1} \right), \quad s^- = \left(\frac{\tilde{\rho}_{2g}\gamma}{g_2} \right). \quad (15)$$

Here αl is weak probe field absorption at the line center and is given by $\alpha l = 4\pi k_p l |d|^2 n / (\hbar\gamma)$; where n denotes the atomic density and l is the length of the cell. For simplicity, we assume $\gamma_1 = \gamma_2 = \gamma$. Under steady state conditions, we solve Eq.(11) to obtain complete analytical solutions for χ_{\pm} or s^{\pm}

$$s^+ = \frac{i\gamma [|G_2|^2 + (\gamma + i(\delta_v - \Omega))(\Gamma_1 + \Gamma_2 + i(\Delta + \delta))]}{|G_2|^2(\gamma + i(\delta_v + \Omega)) + (\gamma + i(\delta_v - \Omega)) [|G_1|^2 + (\gamma + i(\delta_v + \Omega))(\Gamma_1 + \Gamma_2 + i(\Delta + \delta))]}, \quad (16)$$

$$s^- = \frac{i\gamma [|G_1|^2 + (\gamma + i(\delta_v + \Omega))(\Gamma_1 + \Gamma_2 + i(\Delta + \delta))]}{|G_1|^2(\gamma + i(\delta_v - \Omega)) + (\gamma + i(\delta_v + \Omega)) [|G_2|^2 + (\gamma + i(\delta_v - \Omega))(\Gamma_1 + \Gamma_2 + i(\Delta + \delta))]} \quad (17)$$

We note that the atomic velocity dependence of s^{\pm} comes via δ_v . The results presented above are susceptibilities of the atoms moving at \vec{v} . The response of the medium to the input probe field can be obtained by averaging s^{\pm} over the distribution of velocities.

It may be noted that the parameter space in Eqs.(16,17) is very large. Therefore we identify a particular configuration of our interest and work only in the region which gives large asymmetry between $\langle s^+ \rangle$ and $\langle s^- \rangle$, and can lead to large MOR. We focus on a particularly interesting case when $G_2 = 0$; i.e. the control field is σ_+ -polarized ($\mathcal{E}_{c+} = 0$, $\mathcal{E}_{c-} \neq 0$) and it couples the $|1\rangle \leftrightarrow |e\rangle$ transition only. Clearly s^- takes the value that is independent of the control field parameters

$$s^- = \frac{i\gamma}{(\gamma + i(\delta_v - \Omega))}; \quad (18)$$

where as s^+ is strongly dependent on the strength and frequency of the control field

$$s^+ = \frac{i\gamma(\Gamma_1 + \Gamma_2 + i(\Delta + \delta))}{|G_1|^2 + (\gamma + i(\delta_v + \Omega))(\Gamma_1 + \Gamma_2 + i(\Delta + \delta))}. \quad (19)$$

In absence of the control field, the susceptibilities reduce to

$$s^{\pm} = \frac{\gamma}{((\delta_v \pm \Omega) - i\gamma)}; \quad (20)$$

which clearly indicates that s^{\pm} are completely symmetric in absence of magnetic field (i.e. $\Omega = 0$). However, it may be noted from Eq.(18,19) that $s^- \neq s^+$ even in absence of magnetic field, when $|G_1|$ is nonzero. Therefore

electromagnetic field alone can produce birefringence in the medium and hence can cause the plane of polarization of the probe to rotate. This explains the laser field induced birefringence observed in [8,9].

III. SUSCEPTIBILITIES χ_{\pm} OF THE DOPPLER BROADENED MEDIUM

We next calculate the χ_{\pm} of a Doppler broadened medium. Here, as mentioned in Sec.II, one needs to average s^{\pm} over the atomic velocity distribution $\sigma(v_z)$ inside the cell to obtain the response of the medium

$$\langle s^{\pm} \rangle = \int_{-\infty}^{\infty} s^{\pm}(v_z) \sigma(v_z) dv_z. \quad (21)$$

It is assumed that at thermal equilibrium, the atoms in the cell follow Maxwell-Boltzmann velocity distribution

$$\sigma(v_z) = (2\pi K_B T / M)^{-1/2} \exp(-Mv_z^2 / 2K_B T), \quad (22)$$

where mass of the moving atom is M , temperature of the cell T and K_B is Boltzmann constant. For convenience transforming the integral in Eq.(18) from velocity space to frequency space [13], we get

$$\langle s^{\pm} \rangle = \int_{-\infty}^{\infty} s^{\pm}(\delta_v) \sigma(\delta_v) d\delta_v, \quad (23)$$

where the σ distribution in frequency space is

$$\sigma(\delta_v) \equiv \frac{1}{\sqrt{2\pi\omega_D^2}} \exp\left[\frac{-(\delta_v - \delta)^2}{2\omega_D^2}\right]; \quad \omega_D = \omega_{og}(K_B T/Mc^2)^{\frac{1}{2}}. \quad (24)$$

Here ω_D represents the Doppler width in frequency space. For our case of σ_+ control field, we substitute s^\pm from Eqs.(18,19) in Eq.(23) and evaluate the integral. We, thus, obtain the complete analytical results for the Doppler averaged susceptibilities, in terms of complex error functions [14],

$$\langle s^- \rangle \equiv \frac{i\pi\gamma}{\sqrt{2\pi\omega_D^2}} \mathcal{W}\left(\frac{\Omega - \delta + i\gamma}{\sqrt{2}\omega_D}\right); \quad \mathcal{W}(z) = \frac{i}{\pi} \int_{-\infty}^{\infty} \frac{e^{-t^2} dt}{z - t}, \quad (25)$$

$$\langle s^+ \rangle \equiv \frac{i\pi\gamma}{\sqrt{2\pi\omega_D^2}} \mathcal{W}\left(\frac{\zeta - \delta}{\sqrt{2}\omega_D}\right); \quad (26)$$

$$\zeta = i\gamma - \Omega + |G_1|^2/(\Delta + \delta + i(\Gamma_1 + \Gamma_2)).$$

The \mathcal{W} function can be written in terms of the error function $\text{Erf}(x)$

$$\mathcal{W}(\alpha) = e^{-\alpha^2}(1 - \text{Erf}(-i\alpha)); \quad \text{Erf}(z) = \frac{2}{\sqrt{\pi}} \int_0^z e^{-t^2} dt. \quad (27)$$

It may be noted from the argument of \mathcal{W} function in $\langle s^- \rangle$ will show usual Doppler profile since it is independent of the control field but the argument of \mathcal{W} function in $\langle s^+ \rangle$ is strongly dependent on the strength and frequency of the control field and, therefore, the Doppler profile can be modified with these control field parameters.

IV. MEASURE OF ROTATION

Using the $\langle s^\pm \rangle$ obtained above, the rotation of polarization θ of the probe can be determined from Eq.(1) which, however, is valid only if the absorption of the medium is very small. Since we consider the resonant or near-resonant MOR, one also needs to take into account the large absorption associated with the large dispersions near resonance. Absorption contributes to the polarization rotation via dichroism (rotation solely due to $\text{Im} \langle s^\pm \rangle$) but large absorption attenuates the MOR signal at the output.

Let us consider an x -polarized incident probe field propagating along the quantization axis z . The field amplitude can be written as

$$\vec{\mathcal{E}}_{in} = \vec{\mathcal{E}}_p(z=0) = \hat{x}\mathcal{E}_0; \quad (28)$$

which can be resolved into two circularly polarized components as

$$\begin{aligned} \vec{\mathcal{E}}_{in} &= \hat{\epsilon}_+ \mathcal{E}_{p+}(z=0) + \hat{\epsilon}_- \mathcal{E}_{p-}(z=0) \\ &= \frac{\mathcal{E}_0}{\sqrt{2}} (\hat{\epsilon}_+ + \hat{\epsilon}_-). \end{aligned} \quad (29)$$

When the probe field $\vec{\mathcal{E}}_{in}$ passes through the anisotropic medium, $\mathcal{E}_{p\pm}(z)$ evolves. In the limit of a weak probe, we get the output field

$$\vec{\mathcal{E}}_{out} = \vec{\mathcal{E}}_p(z=l) = \frac{\mathcal{E}_0}{\sqrt{2}} \left[\hat{\epsilon}_+ e^{(i\frac{\alpha l}{2} \langle s^+ \rangle)} + \hat{\epsilon}_- e^{(i\frac{\alpha l}{2} \langle s^- \rangle)} \right]. \quad (30)$$

Clearly, $\vec{\mathcal{E}}_{out}$ contains both x and y -polarization components, and thus polarization of the probe is rotated. For small absorption, it is easy to derive the rotation angle θ in Eq.(1). Experimentally one observes the rotation by measuring the intensity after passing the output through a crossed polarizer P_y (as shown in Fig.1) given by

$$T_y = \frac{|(\mathcal{E}_{out})_y|^2}{|\mathcal{E}_{in}|^2} = \frac{1}{4} \left| \exp\left(i\frac{\alpha l}{2} \langle s^+ \rangle\right) - \exp\left(i\frac{\alpha l}{2} \langle s^- \rangle\right) \right|^2; \quad (31)$$

which gives the measure of polarization rotation of the weak x -polarized probe field. Here the intensity of transmission through P_y is scaled with the input intensity in x -polarization. It should be borne in mind that $\langle s^\pm \rangle$ are in general complex.

V. CONTROL OF BIREFRINGENCE AND ENHANCEMENT OF MOR

In this section we identify the regions of our interest and discuss how the control field can be used efficiently to control and hence enhance the MOR. From Eq.(31), one observes the following:

- (i) When $\langle s^+ \rangle \approx \langle s^- \rangle$, $T_y \rightarrow 0$.
- (ii) When $\text{Re} \langle s^+ \rangle \approx \text{Re} \langle s^- \rangle$ but $\text{Im} \langle s^+ \rangle \neq \text{Im} \langle s^- \rangle$, T_y reduces to

$$T_y \simeq \frac{1}{4} \left| e^{(-\frac{\alpha l}{2} \text{Im} \langle s^+ \rangle)} - e^{(-\frac{\alpha l}{2} \text{Im} \langle s^- \rangle)} \right|^2. \quad (32)$$

If both $\frac{\alpha l}{2} \text{Im} \langle s^\pm \rangle$ are large, $T_y \rightarrow 0$. However if $\frac{\alpha l}{2} \text{Im} \langle s^+ \rangle$ is large but $\frac{\alpha l}{2} \text{Im} \langle s^- \rangle$ is small (or vice versa), we obtain

$$T_y \simeq \frac{e^{\alpha l \text{Im} \langle s^- \rangle}}{4} \rightarrow \frac{1}{4}; \quad (33)$$

which is the rotation due to dichroism only.

- (iii) Further when $\text{Im} \langle s^+ \rangle \approx \text{Im} \langle s^- \rangle = \beta$ (say) but $\text{Re} \langle s^+ \rangle \neq \text{Re} \langle s^- \rangle$, we get

$$T_y \simeq \frac{e^{(-\alpha l \beta)}}{4} \left| e^{i\frac{\alpha l}{2} \text{Re} \langle s^+ \rangle} - e^{i\frac{\alpha l}{2} \text{Re} \langle s^- \rangle} \right|^2. \quad (34)$$

If $\alpha l \beta$ is small,

$$T_y \simeq \frac{1}{4} \left| 1 - e^{i \frac{\alpha l}{2} \text{Re}(\langle s^- \rangle - \langle s^+ \rangle)} \right|^2, \quad (35)$$

thus when

$$\frac{\alpha l}{2} \text{Re}(\langle s^- \rangle - \langle s^+ \rangle) = (2n + 1)\pi/2 \quad (n = 0, 1, 2, \dots), \quad T_y = 1. \quad (36)$$

This is the most useful region for our system. This rotation is solely due to birefringence. However if $\alpha l \beta$ is large then $T_y \rightarrow 0$ because this would mean large attenuation of the MOR signal by the medium.

From the above discussion, we have identified that the most interesting frequency region corresponds to very small value of $\text{Im} \langle s^\pm \rangle$ and when the asymmetry between $\text{Re} \langle s^\pm \rangle$ is large. Therefore by selecting the proper control field parameters, one can modify $\langle s^\pm \rangle$ to achieve the objective of large enhancement in MOR. We present below our numerical results and discuss the enhancement of MOR both for stationary atoms and atoms moving according to Maxwellian velocity distribution.

(A) Stationary Atoms

From Eq.(3), the response of the medium, in the limit of stationary atom, is obtained simply by changing $\delta_v \rightarrow \delta$ and $\Delta_v \rightarrow \Delta$. The corresponding susceptibilities (for σ_+ -polarization control field) in Eq.(15,16), thus, reduces to

$$s^- = \frac{i\gamma}{(\gamma + i(\delta - \Omega))}; \quad (37)$$

and

$$s^+ = \frac{i\gamma(\Gamma_1 + \Gamma_2 + i(\Delta + \delta))}{|G_1|^2 + (\gamma + i(\delta + \Omega))(\Gamma_1 + \Gamma_2 + i(\Delta + \delta))}. \quad (38)$$

We present some typical numerical results in Fig.3. In the plots all frequencies are scaled with $\Gamma_1 = \Gamma_2 = \gamma = 1$. The equality is assumed for simplicity. Application of a σ_+ polarized control field modifies s^+ and therefore creates new frequency regions, where s^\pm asymmetry could be large. Thus the result is - large enhancement of MOR signal T_y which is clearly seen in Fig.3. We define the MOR signal enhancement factor be

$$\eta = \frac{(T_y)_{G_1 \neq 0}}{(T_y)_{G_1 = 0}}. \quad (39)$$

For a given δ , η represents the enhancement (if $\eta > 1$) or suppression (if $\eta < 1$) of MOR signal by a control field, when compared to the MOR without control field.

In Fig.3, when the control field is on resonance with $|e\rangle \leftrightarrow |1\rangle$ transition (shown as thick-dashed line), we observe a definite enhancement, at $\delta \simeq -20$. The case of non-resonant control field turns out to be advantageous for larger enhancement of MOR (shown as long-dashed line in Fig.3). For example, at $\delta \simeq -5$ the MOR signal is very high $\sim 70\%$ of the input x -polarized probe intensity, and the corresponding $\eta \simeq 30$. The large MOR,

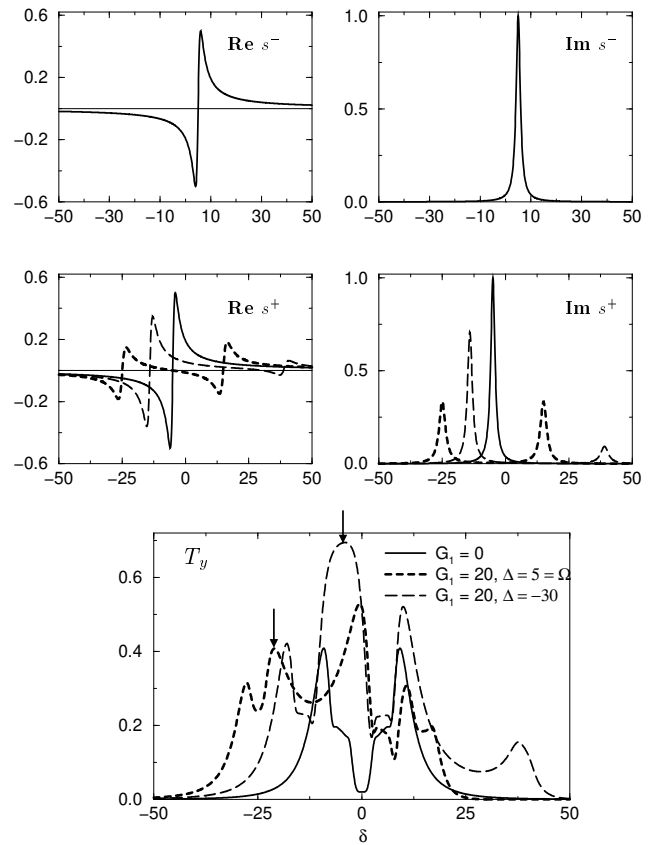


FIG. 3. Field induced birefringence and enhancement of MOR in the stationary atom case is presented as a function of the probe frequency $\delta = (\omega_{og} - \omega_p)/\gamma$. The σ_+ polarized control field modifies s^+ leaving s^- unchanged. Thus the asymmetry between s^\pm is enhanced and hence the MOR. The resonant control field induced changes in s^+ and corresponding T_y s are presented as thick-dashed lines; and that of non-resonant case is presented as long-dashed line. The parameters used in these plots are $\alpha l = 30$ and $2\Omega = 10$. All frequencies are scaled with the natural linewidth γ .

in detuned control laser case, can be attributed to the large asymmetry created between s^\pm due to *the flipping of $\text{Re} s^+$ at these control field parameters*. Similar situation occurs in case of elliptically polarized control field i.e. $G_1 \neq 0 \neq G_2$ (results are not shown here).

(B) Doppler Broadened Medium

In this case large broadening is introduced in both $\langle s^\pm \rangle$ and hence in T_y which is desirable but on the other hand broadening reduces the magnitude of rotation considerably. However, one can work with a denser medium when Doppler effect is included in the calculation. We consider the density such that $\alpha l = 300$. Based on our observations from the analytical results, we present some interesting numerical results for $\langle s^\pm \rangle$ and T_y in Figs.(4)-(6) for different control field parameters so as to achieve control of birefringence and the large enhancement of MOR.

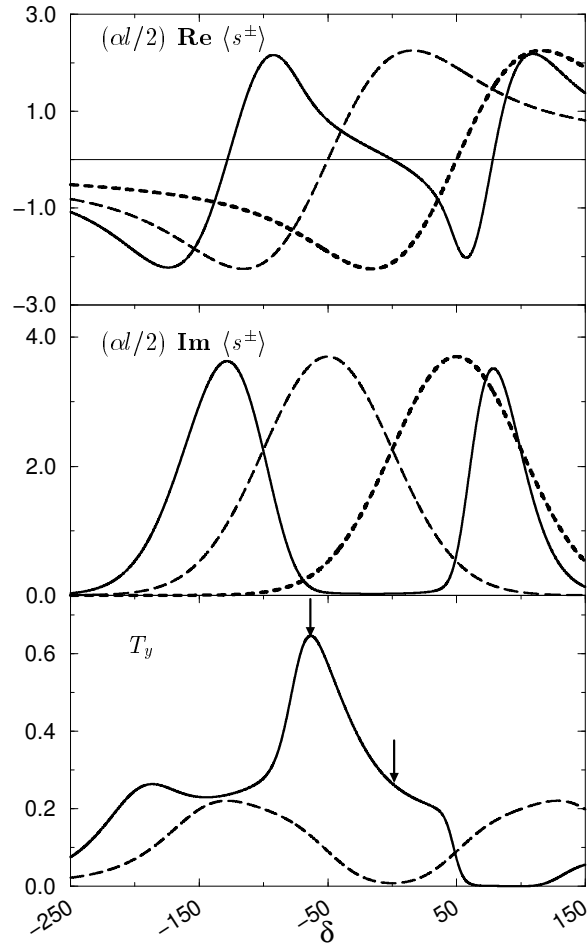


FIG. 4. The enhancements and suppressions of MOR for a control field tuned ($\Delta = 0$) to $|e\rangle \leftrightarrow |i\rangle$ transitions (with $\vec{B} = 0$) with Rabi frequency $G_1 = 100$. In the plots for $\frac{\alpha l}{2}\langle s^\pm \rangle$, the thick-dashed (long-dashed) lines represent $\frac{\alpha l}{2}\langle s^- \rangle$ ($\frac{\alpha l}{2}\langle s^+ \rangle$) in absence of the control field and solid lines represent $\frac{\alpha l}{2}\langle s^\pm \rangle$ in presence of the control field. In the plot for T_y , dashed (solid) curve represents the rotation without (with) control field. The other parameters used are $\omega_D = 50$, $\Omega = 50$. All frequencies are scaled with $\Gamma_1 = \Gamma_2 = \gamma$.

In Fig.4, we consider the effect of an intense control field on resonance with the transition $|e\rangle \leftrightarrow |i\rangle$ (i.e. $\Delta = 0$). We observe enhancement of MOR for certain regions of probe frequencies. In particular we get the enhancement factor $\eta = 34$ for $\delta = 0$. This can be understood as follows- in the absence of the control field and for $\delta = 0$, $\text{Im}\langle s^+ \rangle = \text{Im}\langle s^- \rangle = \beta$ (say) but $\alpha l \beta$ is large, leading to $T_y \approx 0$. However, by application of a control field, the absorption peak is split into two and the minimum of $\text{Im}\langle s^+ \rangle$ appears at $\delta \sim 0$ and hence MOR could be enhanced at this frequency. Further large MOR signal is observed ($T_y \approx 65\%$) at $\delta \approx -63$ which can be attributed to the flipping of the sign of $\text{Re}\langle s^+ \rangle$ causing a large asymmetry between $\text{Re}\langle s^+ \rangle$ and $\text{Re}\langle s^- \rangle$. It may be noted that there are also regions (e.g. for $\delta > 50$) where inhibition of MOR occurs due to large attenuation

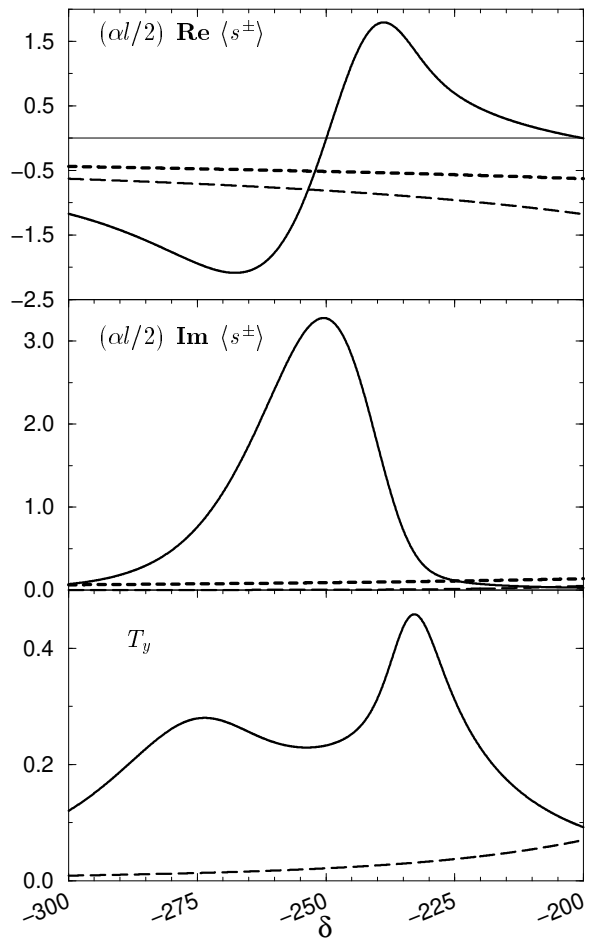


FIG. 5. The enhancement of MOR with a large detuned ($\Delta = 200$) control field. All other parameters are the same as in Fig.4. For prominence, the curve $\frac{\alpha l}{2}\text{Im}\langle s^- \rangle$ is plotted with 50 times their original values. The large enhancement in the region of negative values of δ is shown.

of signal. In Fig.5, the control field strength used is same as in Fig.4 but it is highly detuned ($\Delta = 200$). We present an interesting region which exhibits large MOR, i.e. large T_y . In this region, $\text{Im}\langle s^+ \rangle$ is small due to $\text{Im}\langle s^- \rangle$ electromagnetically induced transparency (EIT) and is small as the probe is far detuned from the atomic center, while at the same time asymmetry between $\text{Re}\langle s^+ \rangle$ and $\text{Re}\langle s^- \rangle$ is large. In Fig.6, we consider the case of a stronger control field. This figure shows large regions of probe frequencies where one obtains significant enhancement of MOR. We also note that the condition (36), for example, is satisfied at $\delta \approx 187.2$, 302.7 (marked by arrows in the Fig.6). However, due to residual absorption, T_y is only equal to 0.8 , 0.27 and the maximum of T_y occurs elsewhere. For $|\delta| > 300$, there is very significant enhancement of MOR; for example at $\delta = -388$, $\eta \approx 140$. Therefore with the crossed polarizer P_y at the output, it is possible to realize a magneto-

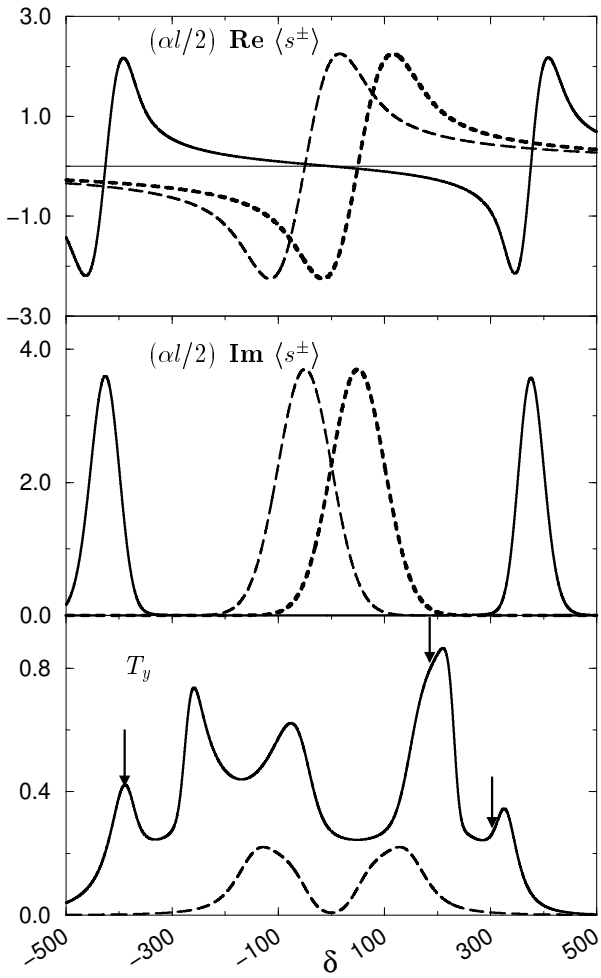


FIG. 6. Significantly large MOR with large enhancements by application of a strong control field ($G_1 = 400$) and $\Delta = 0$. All other parameters and the legends of the curves are same as in Fig.4.

optical switch, that switches the incident polarization to its orthogonal component.

VI. SUMMARY

We have shown how a control field can be used to control birefringence and hence enhance MOR. We have discussed this enhancement in case of stationary atoms as well as moving atoms. We have shown how control laser can modify the susceptibilities and hence one can achieve large enhancement in frequency regions where MOR otherwise is small. The key to large enhancement of MOR consists of utilizing EIT and using probe at frequencies where absorption of both the circularly polarized components is negligible; however, dispersion of the two circularly polarized components is quite different.

Acknowledgment

We thank Prof. J-P. Connerade for the extensive and encouraging discussions on MOR.

- [1] W. Gawlik, J. Kowalski, R. Neumann, H. B. Wiegemann, and K. Winkler, *J. Phys. B* **12**, 3873 (1979); J-P Connerade, *J. Phys. B* **16**, 399 (1983); X. H. He and J-P Connerade, *J. Phys. B* **26**, L255 (1993); X. Chen, V. L. Telegdi, and A. Weis, *Opt. Commun.* **74**, 301 (1990); E. Pfleghaar, J. Wurster, S. I. Kanorsky, and A. Weis, *ibid* **99**, 303 (1993); A. J. Wary, D. J. Heading, and J-P Connerade, *J. Phys. B* **27**, 2229 (1994).
- [2] For extensive discussion on MOR and many interesting applications see: J-P. Connerade, *Highly Excited Atoms*, (Cambridge University Press, 1998); see also W. Gawlik, in “*Modern Non-linear Optics*”, ed. M. Evans, and S. Kielich, *Advances in Chemical Physics Series* vol. LXXXV, Part 3 (Wiley, New York, 1994).
- [3] Magneto-optic effect in transverse magnetic field is discussed in: D. Budker, V. Yashchuk, and M. Zolotorev, *Phys. Rev. Lett.* **81**, 5788 (1998); reduced group velocity in a magneto-optical system is reported in: D. Budker, D. F. Kimball, S. M. Rochester, and V. V. Yashchuk, *Phys. Rev. Lett.* **83**, 1767 (1999).
- [4] M. O. Scully and M. Fleischhauer, *Phys. Rev. Lett.* **69**, 1360 (1992); M. Fleischhauer and M. O. Scully, *Phys. Rev. A* **49**, 1973 (1994); V. A. Sautenkov, M. D. Lukin, C. J. Bednar, G. R. Welch, M. Fleischhauer, V. L. Velichansky, and M. O. Scully, “*Enhancement of Magneto-Optic Effect via Large Atomic Coherence*”, quant-ph/9904032; M. Fleischhauer, A. B. Matsko, and M. O. Scully, “*Quantum limit of optical magnetometry in presence of stark shift*”, quant-ph/0001072.
- [5] G. S. Agarwal, P. Anantha Lakshmi, J-P Connerade, and S. West, *J. Phys. B* **30**, 5971 (1997); P. Jüngner, T. Fellman, B. Stahlberg, and M. Lindberg, *Opt. Commun.* **73**, 38 (1989); K. H. Drake and W. Lange, *ibid* **66**, 315 (1988).
- [6] P. Avan and C. Cohen-Tannoudji, *J. Physique Lett.* **36**, L85 (1975); S. Giraud-Cotton, V. P. Kaftandjian, and L. Klein, *Phys. Rev. A* **32**, 2211 (1985); F. Schuller, M. J. D. MacPherson, and D. N. Stacey, *Opt. Commun.* **71**, 61 (1989).
- [7] For some early studies of field induced birefringence see: P. F. Liao and G. C. Bjorklund, *Phys. Rev. Lett.* **36**, 584 (1976); Y. I. Heller, V. F. Lukin, A. K. Popov, and V. V. Slabko, *Phys. Lett.* **82A**, 4 (1981); A. E. Kaplan, *Opt. Lett.* **8**, 560 (1983).
- [8] B. Stahlberg, P. Jüngner, T. Fellman, K.-A. Suominen, and S. Stenholm, *Opt. Commun.* **77**, 147 (1990); K.-A. Suominen, S. Stenholm, B. Stahlberg, *J. Opt. Soc. America B* **8**, 1899 (1991).
- [9] S. Wielandy and A. L. Gaeta, *Phys. Rev. Lett.* **81**, 3359 (1998); for another recent experiment similar to this one see: F. S. Pavone, G. Bianchini, F. S. Cataliotti, T. W. Hänsch, M. Inguscio, *Opt. Lett.* **22**, 736 (1997).
- [10] S. E. Harris, *Phys. Today*, Pg. 36, July (1997); S. E. Harris, G. Y. Yin, M. Jain, H. Xia, and A. J. Merriam, *Philos. Trans. R. Soc. (London) A* **355**, 2291 (1997).

- [11] A preliminary account of these results has appeared earlier in: A. K. Patnaik and G. S. Agarwal, Opt. Commun. (*in press*); A. K. Patnaik and G. S. Agarwal, in *Frontiers of Laser Physics and Quantum Optics*, Eds. Xu, Xie, Zhu, Scully (Springer-Verlag, Germany) (*in press*).
- [12] Note that the paper [E. L. Lago and R. de la Fuente, Phys. Rev. A **60**, 549 (1999)] reports polarization switching in a Kerr medium.
- [13] W. Demtröder, *Laser Spectroscopy* (Springer, Berlin, 1998), Chap.3. R. Loudon, *The Quantum Theory of Light* (Oxford University Press), Chap.2.
- [14] M. Abramowitz and I. A. Stegun, *Hand Book of Mathematical Functions*, (Dover Publication, NY, 1972), pg. 279.